Available online at www.sciencedirect.com
SCIENCE DIRECT®
Journal of Luminescence 105 (2003) 45–55
JOURNAL OF LUMINESCENCE
www.elsevier.com/locate/jlumin

# Two-photon absorption of tetraphenylporphin free base

Mikalai Kruk[a,b], Aliaksandr Karotki[b], Mikhail Drobizhev[b,c], Valery Kuzmitsky[a], Vladimir Gael[a], Aleksander Rebane[b,*]

[a] *Institute of Molecular and Atomic Physics, National Academy of Sciences, 70 F. Skaryna Ave., 220072 Minsk, Belarus*
[b] *Department of Physics, Montana State University, Bozeman, MT 59717-3840, USA*
[c] *Lebedev Physics Institute, Leninsky Prospekt 53, 119991 Moscow, Russia*

Received 2 December 2002; received in revised form 9 April 2003; accepted 21 April 2003

**Abstract**

We study two-photon absorption (TPA) spectra for toluene solution of 5,10,15,20-tetraphenyl-21H,23H-porphin ($H_2$TPP) in B and Q bands regions and find the maximum TPA cross-section values of 25 and 1–6 GM in laser wavelength ranges, 730–790 and 1100–1400 nm, correspondingly. In the 730–790 nm range the spectrum is attributed to parity allowed two-photon transition into g parity state, positioned nearby B state. Much lower TPA cross-section of $\sim$1 GM is measured for the transition into pure electronic Q state and it is due to the contribution of only those low-symmetry $H_2$TPP confomers, where mutual orientation of the porphyrin plane and the four phenyl rings lifts the center of inversion. The intermediate values of TPA cross-section of $\sim$6 GM are observed for the transition into vibronic Q states and are explained by TPA-allowed transition into vibronic states, which can occur even for totally centrosymmetrical molecules. Measurement of two-photon polarization ratio, $\Omega=\sigma_{circ}/\sigma_{lin}$, shows that for parity allowed g$\rightarrow$g transition $\Omega=1.05\pm0.05$ and for transitions into electronic and vibronic Q-states, $\Omega=0.62\pm0.06$ and $0.79\pm0.1$ (depending on wavelength), respectively. Quantum-chemical calculations of both u and g parity excited energy levels of $H_2$TPP molecule are performed by CNDO/S method and the results are in good agreement with the experimental data.


*PACS:* 42.65.−k; 33.80.Wz

*Keywords:* Porphyrin; Two-photon absorption; Nonlinear spectroscopy of molecules; Quantum-chemical calculations

## 1. Introduction

Two-photon absorption (TPA) has potential practical utility in a variety of areas such as fluorescence microscopy, optical data storage, laser chemistry, micro-fabrication and photo-medicine (Refs. [1–8] and References therein). Application of porphyrins is especially attractive in TPA-based photodynamic therapy, where the reduced absorption and scattering at near infrared wavelengths has the advantage of deeper penetration of light in body tissues [8,9].

Recently, we showed that TPA cross-section of some porphyrins can reach $\sigma_2$ $\sim$100–1000 GM

*Corresponding author. Tel.: +1-406-994-7831; fax: +1-406-994-4452.
*E-mail address:* rebane@physics.montana.edu (A. Rebane).

0022-2313/03/$ - see front matter 
doi:10.1016/S0022-2313(03)00096-6

(1 GM (Goeppert–Meyer) $= 1 \times 10^{-50}$ cm$^4$ s/photon) in the Soret band region [10,11]. We demonstrated that $\sigma_2$ in some porphyrins is sufficiently large also for effective photosensitization of singlet molecular oxygen at near infrared wavelengths range [10]. We gave a tentative explanation of the large $\sigma_2$ value as resulting from resonance enhancement effect, which occurs if the excitation wavelength is close to Q band one-photon transition of the porphyrin. In symmetrically substituted porphyrins we also observed TPA enhancement due to transition to g parity excited states in Soret region [11].

In spite of this recent progress in experimental investigations, systematic spectroscopic analysis of TPA of the tetrapyrrolic compounds is still lacking. In this paper we present, for the first time, the detailed experimental and quantum-chemical study of the TPA by 5,10,15,20-tetraphenyl-21H, 23H-porphin ($H_2$TPP). We choose this compound because it is one of the fundamental structures in the family of tetrapyrrolic molecules [12]. The TPA spectra in both visible and UV regions of transition wavelength are reported along with measurements of the TPA polarization ratio. We carry out quantum-chemical calculations of excited electronic states of $H_2$TPP and compared the theoretical results with our experimental findings concerning two-photon allowed transitions into g parity excited states.

## 2. Experimental details and methods of calculations

5,10,15,20-Tetraphenyl-21H, 23H-porphine was purchased from Aldrich and was used as received. We carefully examined its absorption and fluorescence and found that there was no evidence of either chlorin derivative or some other impurities. Toluene (spectroscopic grade) was obtained from Sigma. All the experiments were carried out in standard spectroscopic $1 \times 1$ cm$^2$ rectangular quartz cells in the air-equilibrated solutions at room temperature. Porphyrin concentration was $\sim 1 \times 10^{-5}$ M and was determined spectrophotometrically from known extinction coefficients [13].

The laser system has been already described [10,11]. Ti: Sapphire regenerative amplifier (CPA-1000, Clark, MXR) was operated at 1 kHz repetition rate and produced 150-fs long pulses (FWHM) of 0.8 mJ per pulse at $\lambda = 780$ nm. The pulses were parametrically down-converted in the optical parametric amplifier (TOPAS, Quantronix), which yielded 100-fs long pulses (FWHM) in the wavelength range from 1.1 to 1.6 μm, with energy 100–200 μJ per pulse. The laser spectrum was recorded with either Lambda 900 Perkin-Elmer spectrophotometer coupled with a light-collecting fiber or with TRIAX 550 Jobin Yvon/Spex spectrometer. Pulse duration and its temporal profile for both regenerative and optical parametric amplifiers were measured with autocorrelator. Porphyrin fluorescence was collected and focused with a spherical mirror on the entrance slit of TRIAX 550 Jobin Yvon/Spex spectrometer and then was measured with photomultiplier.

Absolute value of $\sigma_2$ was evaluated by measuring fluorescence intensity under one- and two-photon excitation, as described in Refs. [4,10,11]. In the 700–800 nm excitation wavelength region $\sigma_2$ was measured at 780 nm. Fundamental wavelength ($\lambda = 780$ nm) of Ti–sapphire regenerative amplifier and its second harmonic ($\lambda = 390$ nm) were used for two- and one-photon excitation, correspondingly. The TPA spectra were obtained by tuning the optical parametric amplifier with subsequent second harmonic generation. The resulting spectra were scaled to the measured absolute value at one wavelength. In two-photon polarization ratio $\Omega = \sigma_{circ}/\sigma_{lin}$ measurement, linearly polarized light was converted to circularly polarized light by using a quarter-wave plate ($\lambda$/4-plate).

In the 1.1–1.4 μm spectral region optical parametric amplifier was used for both TPA cross-sections and spectra measurements. In the TPA spectra measurements the laser beam was focused by $f = 25$ cm lens, in case of $\sigma_{TPA}$ measurements $f = 50$ cm lens was used. The sample was placed out of the focus. Pinhole was placed just before the sample to insure that radii of pinhole and beam in the sample are the same.

Quantum-chemical calculations were carried out for $H_2$TPP and free base porphin (hereafter referred as $H_2$P), where the last was taken for comparison to elucidate the role of substitution on

the excited states energy. The calculations were done in two stages. At first, the geometry optimization of the $H_2P$ and $H_2TPP$ molecules in their ground state was carried out. The AM1 method [14] in the MOPAC6 software package [15] was used. The initial atomic coordinates for $H_2P$ and $H_2TPP$ were taken from average X-ray data [16,17]. In the second stage, the calculations of the exited electronic states were performed by the CNDO/S method [18,19]. The configuration interaction with the single electron excitations (CIS) was used. The CIS included the following numbers of configurations (occupied MOs × unoccupied MOs): $13 \times 15 = 195$ and $29 \times 31 = 899$ for $H_2P$ and $H_2TPP$, respectively. Software package used in these calculations was designed in our group. The electronic density redistribution upon excitation was calculated using transition density matrix formalism [20,21]. With this approach, the probabilities of the excitation localization on the given fragments of a molecule as well as that of electron transfer between them were determined. The porphyrin macrocycle (P) and four phenyl rings (B) were chosen as the fragments for $H_2TPP$ molecule.

## 3. Results and discussion

The TPA spectra of $H_2TPP$ together with its one-photon linear absorption spectra are shown at Fig. 1. TPA spectra do not match with the linear one-photon absorption spectra in the whole spectral range studied. Therefore we will discuss the data found for Soret and Q bands regions separately.

### 3.1. Experimental TPA spectra in Q band region

In the Q-band region (Fig. 1b), TPA bands correspond to one-photon absorption bands, but they are broadened and red-shifted. Comparison of TPA bands centered at ~600 and ~660 nm with corresponding one-photon absorption bands shows that two-photon transition into vibronic Q(0,1) state is enhanced as compared to that into pure electronic Q(0,0) state. The intensity ratio for two-photon transition, $I_{660}/I_{600} \sim 2/10$, whereas for one-photon transition, $I_{Q(0,0)}/I_{Q(0,1)}$ is only about 2/3. This behavior is not surprising, if we assume that $H_2TPP$ has center of symmetry: two-photon transition into pure electronic u parity Q(0,0) state is parity forbidden since ground state is of g parity. Prohibition can be removed because of the molecular symmetry distortions due to nonsymmetrical vibrations and solvent influence [22]. In the case under consideration, distortion of the symmetry may arise from interaction between the porphyrin macrocycle and the four phenyl substituents in the *meso*-carbon positions. It is generally accepted that phenyl rings in $H_2TPP$ and its metalloderivatives are noncoplanar with

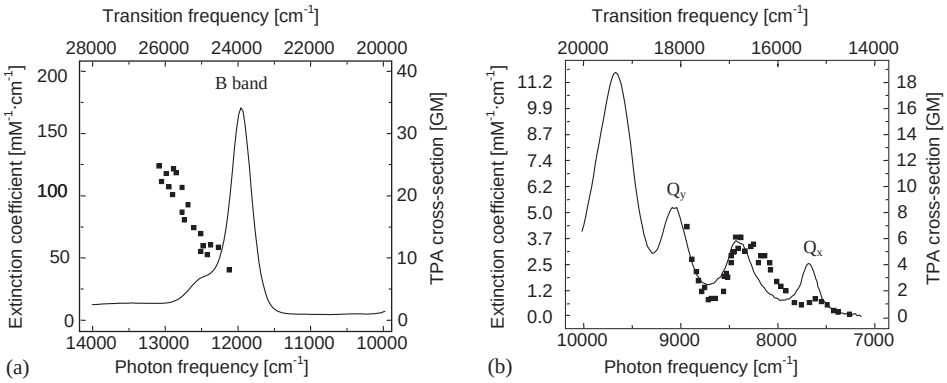


Fig. 1. $H_2TPP$ TPA spectrum (■) and one-photon linear absorption spectrum (line) in the visible (a) and UV (b) regions of the transition frequency. Top and bottom abscisses are the transition and the laser frequencies, respectively. Left and right ordinates are the linear extinction coefficient (in $mM^{-1}\,cm^{-1}$) and the TPA cross-section (in GM), respectively.

the porphyrin plane [23–25]. Dihedral angle $\Theta$ between the mean porphyrin plane and the plane of phenyl ring is about 60° [23–25] and the geometry optimization done in this work gives $\Theta = \pm 63°$ for the opposite phenyl rings. Note that along with the optimized center-symmetric structure shown in Fig. 2a, there are possible other structures with about the same minimum energy, but without the center of inversion (see below). Since the phenyls are the main symmetry-distorting factor, we conclude that these groups must also contribute most to TPA. Thus, the observation of the TPA transition into Q(0,0) state in $H_2TPP$ molecule indicates that the actual symmetry is lower than $D_{2h}$, usually attributed to free base porphyrin ring. In all, the TPA cross-section does not exceed 1–6 GM over the whole Q band range studied, and has the same order of magnitude as reported earlier for other tetrapyrrolic compounds [4,10,26].

The coupling between electronic and vibrational wavefunctions, which is different for one- and two-photon transitions, must cause the increase of TPA in vibronic band. Indeed, fluorescence line narrowing experiments and theoretical considerations have shown that Q(0,1) vibronic band is formed due to both g and u parity vibrations, assuming the molecule is centrosymmetrical [27]. In this case, parity of the vibronic wavefunction results from parities of electronic and vibrational wave functions. Since, for the first excited Q state, the electronic moiety is of u parity, its combination with u parity vibrational wavefunction leads to overall g parity state: $\psi_u\chi_u = \Phi_g$. Therefore, two-photon transition into vibronic Q(0,1) state should be considered as allowed one, which explains its relatively high intensity as compared to pure electronic Q(0,0) state. We note that similar situation is well known in one-photon spectroscopy, where the parity forbidden electronic transitions have been allowed by vibronic coupling [22,27]. The intensity of such transition is lower than intensity of totally allowed transition by a factor of, $\omega_{vib}/\omega_{el}$, where $\omega_{vib}$ and $\omega_{el}$ are the frequencies of the molecular vibrations and electronic transitions, respectively.

### 3.2. Experimental TPA spectra in Soret band region

Fig. 1b shows that the TPA spectrum of the $H_2TPP$ in the UV range of the transition wavelength is completely different from the linear one-photon spectrum. Above we described two mechanisms, which can lift the prohibition by parity for two-photon transitions in Q band

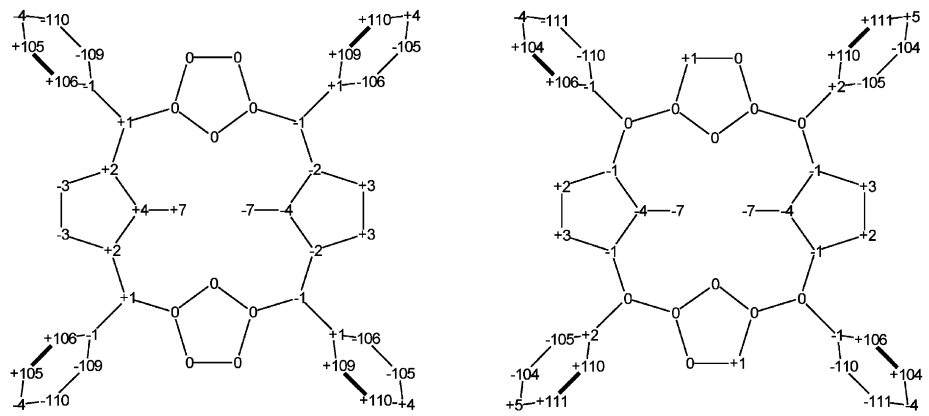


Fig. 2. The out-of-plain displacements for the $H_2TPP$ atom centers (in Å × 100) from the mean plane of porphin macrocycle in accordance with the geometry optimization results: (a) $C_{2h}$ symmetry constrains; (b) $C_2$ symmetry constrains. For $H_2TPP$ molecule ($C_{2h}$) $C_2$ axis goes through nitrogen atoms of the pyrrolenyne rings and for $H_2TPP$ molecule ($C_2$) $C_2$ axis is perpendicular to the mean plane of the porphyrin macrocycle.

region, namely, lowering of the molecular symmetry and the vibronic origin of transitions. However, in the case under consideration both these mechanisms are less important because TPA cross-section in Soret band region is already about one order of magnitude larger. Nearly monotonic increase of $\sigma_2$ towards higher frequency (as well as rather high cross-section values up to 25 GM) can be explained by the presence of allowed two-photon transitions, which turn out to be lying higher than B state. It is known from the estimation made for the long-chain linear polyenes [28], that TPA cross-section for parity allowed two-photon transition does not exceed 10 GM. Higher values found for $H_2$TPP suggest that TPA enhancement mechanisms in case of tetrapyrrolic compounds are much stronger.

Measurements of transient stepwise absorption in several porphyrins, including $H_2$TPP [29–31], show no distinct $S_1 \rightarrow S_n$ absorption band in the near-IR (near-IR absorption from $S_1$ state probes the same spectral range as UV absorption from the ground $S_0$ state), but only a smooth absorption tail, monotonically increasing towards higher energies. Quantum-chemical calculations carried out for different porphyrin molecules reveal a number of g parity excited states near and above B state [32–36].

The results for $H_2$TPP are in a good agreement with those reported recently for other porphyrin molecules where the enhancement of the TPA cross-section in the Soret band region has been also explained by the parity allowed g→g transition [10,11,37,38]. Thus, for 5,15-diphenylporphyrin free base the $\sigma_2$ value at excitation wavelength 750 nm was found to be 12 GM but when one of the phenyl groups was substituted for 4-diphenylaminostilbene one, $\sigma_2$ value edged up to 80 GM [10]. In tetraazaporphyrins symmetrically substituted with strong electron accepting groups the further enhancement up to $\sigma_2 \sim 1600$ GM has been found [37]. For the free base tetrabenzoporphyrin the $\sigma_2$ value of 20 GM at 780 nm was found and in the series of Zn–tetrabenzoporphyrins with the sequential substitution of phenyl groups in the meso-positions the value of TPA cross-section $\sigma_2$ was measured ranging from 50 GM in case of diphenyl substituted derivative up to 130 GM in case of tri-phenyl substituted molecule [11]. Metallo-derivatives of the tetrakis-trimethoxyphenylporphyrin revealed the $\sigma_2$ value of 31–114 GM at the excitation wavelength 840 nm, depending on the nature of the embedded metal ion [38].

Thus, the measured TPA spectrum can be attributed to several overlapping g→g transitions, giving rise to broad TPA absorption band. For all the experimental data points shown in Fig. 1 we attested that the two-photon excited fluorescence does have a quadratic dependence on laser power. At higher excitation frequencies, this dependence starts to transform gradually into linear one because of onset of the one-photon absorption. This experimental circumstance prevents us from extending of spectral range of TPA measurements deeper in UV.

We should stress that the frequency of the excitation photons in this spectral region is close to the frequency of the one-photon allowed Q transitions. Thus, the resonance enhancement due to small detuning between frequencies of excitation photons and one-photon transition can contribute into TPA cross-section. Recently we demonstrated that for some porphyrins high values of TPA cross-section contain an important contribution from the resonance enhancement effect [11]. Therefore, the values of TPA cross-section in UV-range should be regarded as values for g→g two-photon transition with an endowment of the resonance enhancement. As one can see at Fig. 1a, the maximum of this new TPA band was somewhat higher in energy than we could reach. Moderate TPA cross-section values obtained in the accessible spectral range can be explained by large detuning from that of actual g→g absorption maximum. Quantum-chemical calculations support this assumption (see below).

### 3.3. Measurements of TPA polarization ratio

It is known that two- and one-photon spectroscopy differ markedly with respect to polarization phenomena. Two-photon spectroscopy can provide absolute symmetry assignment for electronic states using samples consisting of randomly oriented molecules (e.g. solution), whereas performing of the same task with one-photon

spectroscopy requires rigid samples with uniformly oriented molecules [39]. In practice, it is convenient to measure the ratio of TPA cross section for circularly polarized light versus linearly polarized light, $\Omega = \sigma_{circ}/\sigma_{lin}$. The TPA polarization ratio for a two-photon allowed transition in molecules (single laser source) typically falls in the range $\frac{2}{3} \leqslant \Omega \leqslant \frac{3}{2}$ [22,39]. An additional useful feature is that within two-photon allowed electronic (vibronic) absorption band $\Omega$ does not depend on the wavelength, and is determined by the symmetry of the pure electronic state only [22]. This fact allows us to measure $\Omega$ at a few wavelengths only. At the transition wavelength 390 nm we find $\Omega = 1.05 \pm 0.05$. This result is in a good agreement with the theoretical $\Omega$ value derived from calculations [33], where $\Omega \sim 1.0$ was obtained for allowed TPA transitions in porphyrin molecules with "$D_{2h}$-like" symmetry. For two-photon "forbidden" transitions, i.e. for the transitions into Q states, on the other hand, $\Omega$ depends on the frequency within the given vibronic band, and can vary from $\frac{1}{4}$ to $\frac{3}{2}$ [22,39]. For the transition wavelengths 572.2, 597.0, 624.0 and 655.0 nm, we obtained $\Omega$ values $0.62 \pm 0.06$, $0.71 \pm 0.1$, $0.79 \pm 0.1$, $0.79 \pm 0.1$, respectively. The fact that these values are lower than that measured in UV range, and that $\Omega$ depends on the wavelength, can be considered as evidence in support of the notion that the transitions into Q states are of different origin.

### 3.4. Theoretical results: optimization of molecular geometry

As far as we know, $H_2$TPP excited states have not been considered by quantum-chemical methods. The results concerning the porphyrin g parity "hidden" excited states are fragmentary and incomplete, only few reliable papers can be cited [32,33].

We begin the discussion of our quantum-chemical calculations by considering geometry optimization protocol, where the initial symmetry constrains are $D_{2h}$ and $C_{2h}$ for $H_2$P and $H_2$TPP. respectively. Results for $H_2$P agree well with the calculations [40], which were performed without symmetry constrains. Fig. 2a shows how much individual atoms deviate from the mean porphyrin plane in case of $H_2$TPP. It is seen that the porphyrin macrocycle is practically planar, whereas the pyrrolenyne rings are in the median plane of the macrocycle. The most pronounced are the out-of-plane deviations of the pyrrole rings, but they are also only about 0.1 Å. The plane perpendicular to the pyrrole ring makes a $\sim 2^\circ$ angle with that of the mean porphyrin plane. The pyrrole rings are titled out of mean porphyrin plane about an axis lying in the plane and passing near midpoint of two $C_a$–$C_b$ bonds. The same pattern of the distortions in $H_2$TPP has been observed by the X-ray diffraction [17], but the deviations had somewhat larger values. Taken separately, all four pyrrole and phenyl rings are planar. The dihedral angle between the phenyl planes and mean porphyrin plane is about 63°. The mutual orientation of the phenyl rings corresponds to that derived from X-ray data [17].

As was pointed out earlier, if we assume that $H_2$TPP has no center of inversion, then the parity selection rule does not hold exactly. To clarify this situation, we carried out AM1 geometry optimization with $C_2$ symmetry constraints. The resulting structure is presented in Fig. 2b. The only essential difference consists in the dihedral angle between the phenyl ring and the mean porphyrin macrocycle planes of the opposite phenyl groups. In case of $C_{2h}$ symmetry (with center of inversion), these angles are 63° and −63°, whereas for the $C_2$ symmetry (no center of inversion) both angles are 63°. These two structures revealed negligibly small differences in the energy. Moreover, in the recent paper [41] a number of $H_2$TPP conformers has been calculated ab initio at BPW91/6-31G* level. All these conformers differ only by orientation of the phenyl rings ($\Theta = \pm 65$–$70^\circ$) and the energy difference between all these structures is negligibly small (maximum energy difference among them is 1.4 kcal/mol). These results demonstrate that porphyrin macrocycle interacts with each of phenyl rings independently. In fact, there exists a certain set related structures, where the dihedral angles between the porphyrin mean plane and the phenyl rings are $\pm 60$–$70^\circ$. It should be noted that $^1$H NMR data indicate that at the temperatures of few tens degrees above room temperature a rather

fast rotation of phenyl rings (up to $100\,s^{-1}$) takes place [42]. Therefore, we conclude that not all, but only those $H_2TPP$ molecules, which do not have the center of inversion, contribute to the pure electronic Q(0,0) band in the TPA spectrum.

### 3.5. Theoretical results: energy levels calculation

The MO calculation results for the $H_2P$ ($D_{2h}$) and $H_2TPP$ ($C_{2h}$) molecules are listed in Table 1. The two lowest unoccupied MOs $\varphi_2$ ($4b_{3g}\rightarrow 27b_g$) and $\varphi_1$ ($4b_{2g}\rightarrow 31a_g$) do not change appreciably their energy when going from $H_2P$ to $H_2TPP$. At the same time, the energy of the highest occupied MO, $\varphi_{-1}$ ($2a_u\rightarrow 27a_u$) decreases by 0.1 eV. These MOs of $H_2TPP$ are strongly localized on the porphyrin part of molecule ($\ell_P = 95$–$99\%$). However, the energy of $\varphi_{-2}$ ($5b_{1u}\rightarrow 30b_u$) does increase significantly, by 0.47 eV. This is due to the fact that $\varphi_2$ ($5b_{1u}$) of $H_2P$, as well as the corresponding $a_{2u}$-symmetry MO [43], has antinodal points on the carbon *meso*-atoms $C_m$. Upon attachment of the phenyl rings to the porphyrin macrocycle, this MO obtains antibonding character along the $C_m$–$C_{Ph}$ bonds (see also Refs. [25,44]). As a consequence, $7a_u$ and $30b_u$ MOs of $H_2TPP$ are almost degenerate ($\Delta\varepsilon = 0.13$ eV), while the gap $\Delta\varepsilon$ between 3au and $5b_{1u}$ of $H_2P$ is 0.60 eV. As compared to $H_2P$, adding the phenyls in $H_2TPP$ bring about MOs, which are localized on the phenyl rings. In particular, two highest occupied doubly degenerate MOs $e_{1g}$ of a benzene molecule give Eight one-electron states. Similarly, two lowest unoccupied doubly degenerate MOs $e_{2u}*$ give Eight one-electron states. Part of these phenyl-localized MOs levels is listed in Table 1.

Table 1
Orbital energy (in eV) of the $H_2P$ and the $H_2TPP$ molecules

| $H_2TPP$ | | | | $H_2P$ | | |
|---|---|---|---|---|---|---|
| No. | Sym. | ε | $\ell_P$ (%)[a] | No. | Sym. | ε |
| *Lower unoccupied MOs*[b] | | | | | | |
| 12 | $33b_u$ | −0.27 | 75 | 4 | $6b_{1u}$ | −0.29 |
| 11 | $30a_u$ | −0.43 | 18 | | | |
| 10 | $29b_g$ | −0.47 | 5 | | | |
| 9 | $33a_g$ | −0.52 | 1 | | | |
| 8 | $32b_u$ | −0.52 | 0 | | | |
| 7 | $29a_u$ | −0.53 | 1 | | | |
| 6 | $28b_g$ | −0.53 | 1 | | | |
| 5 | $32a_g$ | −0.55 | 8 | | | |
| 4 | $31b_u$ | −0.58 | 28 | | | |
| 3 | $28a_u$ | −1.13 | 84 | 3 | $3a_u$ | −1.07 |
| 2 | $27b_g$ | −2.69 | 95 | 2 | $4b_{3g}$ | −2.71 |
| 1 | $31a_g$ | −2.87 | 98 | 1 | $4b_{2g}$ | −2.86 |
| *Higher occupied MOs*[c] | | | | | | |
| −1 | $27a_u$ | −7.27 | 99 | −1 | $2a_u$ | −7.17 |
| −2 | $30b_u$ | −7.40 | 89 | −2 | $5b_{1u}$ | −7.87 |
| −3 | $30a_g$ | −9.27 | 33 | | | |
| −4 | $26b_g$ | −9.32 | 27 | | | |
| −5 | $26a_u$ | −9.47 | 10 | | | |
| −6 | $25b_g$ | −9.51 | 93 | −3 | $3b_{3g}$ | −9.54 |
| −7 | $29b_u$ | −9.52 | 59 | −4 | $4b_{1u}$ | −9.68 |
| −8 | $28b_u$ | −9.75 | 43 | | | |
| −9 | $29a_g$ | −9.89 | 7 | | | |
| −10 | $24b_g$ | −9.92 | 7 | | | |
| −11 | $25a_u$ | −9.94 | 2 | | | |
| −12 | $27b_u$ | −9.94 | 13 | | | |

[a] Degree of the localization on the porphyrin macrocycle (%). Degree of the localization on four phenyl rings is $1-\ell_P$.
[b] Unoccupied MOs are given with positive numbers.
[c] Occupied MO are given with negative numbers.

The calculation results of the excited states of the $H_2P$ and $H_2TPP$ molecules are presented in Table 2. The data are presented for the optimized structures $H_2P$ ($D_{2h}$) and $H_2TPP$ ($C_{2h}$). $H_2TPP$ structures optimized with $C_2$ and $C_{2h}$ constrains give the same ordering of the excited states. The energies of all states relevant in this study differ by no more than $20\,cm^{-1}$. We should note that our results for $H_2P$ on both u and g excited states reproduce data of earlier calculations by CNDO/S-CIS [32,45] as well as INDO/S-CIS [46]. Our calculations appear to agree reasonably well also with results obtained by ab initio methods [35]. The lowest exited states of odd symmetry $1^1B_{3u}$, $1^1B_{2u}$ (or $Q_x$, $Q_y$) of $H_2P$ are determined by the contributions of the electronic $\pi\pi^*$ configurations $\varphi_{-1}\varphi_1$, $\varphi_{-1}\varphi_2$, $\varphi_{-2}\varphi_1$, $\varphi_{-2}\varphi_2$ (Gouterman's four orbital model [43]). The $Q_x$ and $Q_y$ states of $H_2TPP$ remain to be localized on the porphyrin part of the molecule (Table 2). These levels undergo bathochromic shifts, 800 and $600\,cm^{-1}$, respectively, which agrees with experimental data for vapors, where the corresponding shift was 850 and $1200\,cm^{-1}$ [47].

Since intense TPA is observed nearby Soret band it is worthwhile to discuss in details the calculation results on the structure of the excited

Table 2
Energy ($10^3\,cm^{-1}$) and oscillator strength of the $H_2TPP$ and $H_2P$ molecules

| $H_2TPP$ | | | | | | $H_2P$ | | | |
|---|---|---|---|---|---|---|---|---|---|
| State | $E_{calc}$ | $f$ | φ, θ[a] | $L_{AB}$[b] (%) | $E_{exp}$[c] | State | $E_{calc}$ | $f$ | $E_{exp}$[c] |
| $1^1B_u\ Q_x$ | 13.0 | $3.10^{-4}$ | 0,123 | 93P | 15.1 | $1^1B_{3u}\ Q_x$ | 13.8 | 0.04 | 15.95 |
| $1^1A_u\ Q_y$ | 15.8 | 0.02 | 90,90(*y*) | 93P | 18.3 | $1^1B_{2u}\ Q_y$ | 16.4 | 0.17 | 19.5 |
| $2^1B_u\ B_x$ | 25.6 | 2.81 | 0,91 | 88P | 24.8 | $2^1B_{3u}\ B_x$ | 26.9 | 1.78 | 26.8 |
| $2^1A_u\ B_y$ | 25.9 | 3.23 | 90,90(*y*) | 84P | | $2^1B_{2u}\ B_y$ | 28.7 | 2.59 | |
| $1^1B_g$ | 28.6 | 0 | | 95P | | $1^1B_{1g}$ | 28.7 | 0 | |
| $2^1A_g$ | 28.7 | 0 | | 92P | | $2^1A_g$ | 28.9 | 0 | |
| $3^1B_u\ N_x$ | 30.9 | 0.85 | 0,91 | 85P | | $3^1B_{3u}\ N_x$ | 32.6 | 1.73 | 29.4 |
| $2^1B_g$ | 31.7 | 0 | | 79P | | $2^1B_{1g}$ | 33.6 | 0 | |
| $3^1A_g$ | 32.8 | 0 | | 48P + 48BP | | | | | |
| $3^1B_g$ | 33.4 | 0 | | 39P + 58BP | | | | | |
| $4^1B_g$ | 33.8 | 0 | | 54P + 33BP | | | | | |
| $3^1A_u$ | 34.9 | 0.09 | 90,90(*y*) | 44P + 50BP | | | | | |
| $4^1A_g$ | 35.1 | 0 | | 82P | | $3^1A_g$ | 35.0 | 0 | |
| $4^1B_u$ | 35.3 | 0.09 | 0,51 | 43P + 53BP | | | | | |
| $5^1A_g$ | 35.5 | 0 | | 33P + 6BP | | | | | |
| $5^1B_g(n\pi^*)$ | 35.5 | 0 | | 80P | | $1^1B_{3g}(n\pi^*)$ | 35.6 | 0 | |
| $4^1A_u\ N_y$ | 35.6 | 0.06 | 90,90(*y*) | 54P + 40BP | | $3^1B_{2u}\ N_y$ | 36.0 | 0.40 | |
| $6^1B_g$ | 35.9 | 0 | | 64P | | | | | |
| $5^1B_u(n\pi^*)$ | 36.0 | 0.05 | 0,124 | 48P + 23B | | $1^1B_{1u}(n\pi^*)$ | 36.1 | 0.12 | |
| $6^1A_g$ | 36.1 | 0 | | 31P + 34PB | | | | | |
| $5^1A_u$ | 36.1 | 0.00 | 90,90(*y*) | 49B + 37B | | | | | |
| $7^1B_g$ | 36.3 | 0 | | 60B | | | | | |
| $6^1B_u$ | 36.3 | 0.12 | 0,22 | 29P + 39B | | | | | |
| $7^1A_g$ | 36.4 | 0 | | 36B + 33PB | | | | | |
| $7^1B_u$ | 36.5 | 0.00 | 0,164 | 70PB | | | | | |
| $6^1A_u$ | 36.7 | 0.00 | 90,90(*y*) | 68PB | | | | | |
| $8^1A_g$ | 37.5 | 0 | | 73PB | | | | | |
| $8^1B_u$ | 37.7 | 0.11 | 0,89 | 67BP | | | | | |
| $7^1A_u$ | 37.8 | 0.05 | 90,90(*y*) | 76PB | | | | | |
| $9^1B_u$ | 37.9 | 0.03 | 0,68 | 87PB | | | | | |
| $8^1B_g$ | 37.9 | 0 | | 33P + 57PB | | $3^1B_{1g}$ | 37.8 | | |
| $9^1B_g$ | 38.0 | 0 | | 76PB | | | | | |
| $9^1A_g$ | 38.2 | 0 | | 55P + 34PB | | $3^1A_g$ | 38.5 | | |
| $8^1A_u$ | 38.3 | 0.09 | 90,90(*y*) | 30P + 50BP | | | | | |
| $10^1A_g(n\pi^*)$ | 38.6 | 0 | | 67P + 27PB | | $1^1B_{2g}(n\pi^*)$ | 38.1 | | |
| $11^1A_g$ | 38.7 | 0 | | 87PB | | | | | |
| $10^1B_u$ | 38.7 | 0.00 | 0,98 | 93PB | | | | | |
| $9^1A_u(n\pi^*)$ | 38.7 | 0.00 | 90,90(*y*) | 46P + 45PB | | $1^1A_u(n\pi^*)$ | 38.5 | | |

[a] $\varphi$, $\theta$ are the polar coordinates of transition dipole moment vector.
[b] Probabilities of local excitations of fragments P and B, and electron transfer excitations from P to B or from B to P, where P stands for porphyrin macrocycle and B stands for four phenyl rings. Only main contributions are given.
[c] Experimental vapor data are taken from Edwards et al. [47].

states in near UV region. For $B_x$, $B_y$, $N_x$ states the following features can be noted: (i) all these states are localized on porphyrin macrocycle, but the degree of localization (84–88%) is less than that for $Q_x$ and $Q_y$ states (93%); (ii) transitions from the ground state (hereafter denoted as G) $G \rightarrow B_x$, $G \rightarrow B_y$, $G \rightarrow N_x$ are shifted towards lower frequency, by 1300, 2800 and 1700 $cm^{-1}$. The experimental shift of Soret band makes up 2000 $cm^{-1}$; (iii) The energy gap between $B_y$ and $B_x$ levels lowers from 1800 to 300 $cm^{-1}$; (iv) The transition $G \rightarrow N_x$ loses intensity by the factor of

two and can be related to the shoulder observed at the short wavelength side of the Soret band [47]. This behavior of the $G \rightarrow B_x$, $G \rightarrow B_y$, and $G \rightarrow N_x$ transitions for $H_2TPP$ as compared to $H_2P$ is due to shifting of two upper filled levels, $\varphi_{-1}$, $\varphi_{-2}$, especially increase of energy of $\varphi_{-2}$ level. Thus, our results confirm that the four orbital model is applicable to $H_2TPP$, and even more so than to $H_2P$. We note that in the high energy region, above 35,000 $cm^{-1}$, our calculations yield u symmetry states of a mixed nature, where the excitation can be localization on the porphyrin macrocycle as well as have a charge transfer character, mainly of $B \rightarrow P$ type (see also Refs. [25,44]).

The calculations for $H_2P$ give in a range of 28,000–38,000 $cm^{-1}$ six $\pi\pi^*$ states of g parity: $1^1B_{1g}$, $2^1A_g$, $2^1B_{1g}$, $3^1A_g$, $3^1B_{1g}$, $4^1A_g$ (see Table 2). Also in this region are four $n\pi^*$ levels, of which three are of g type. Two low-lying levels, $1^1B_{1g}$ and $2^1A_g$ are somewhat above $B_y$ level (30 and 200 $cm^{-1}$). The main configuration of the $1^1B_1g$ state is either $\varphi_{-3}\varphi_1$ or $4b_{3g}4b_{2g}$ ($k_{CIS} = 0.92$). The $2^1A_g$ state is predominantly determined by the $\varphi_{-1}\varphi_3$ or $2a_u3a_u$ configuration, $k_{CIS} = 0.91$.

Our results on $H_2P$ can be compared with the ab initio calculations reported in Ref. [35]. First, ab initio methods give the same ordering of the six g parity $\pi\pi^*$ states. Moreover, our computed energy of the lowest excited g parity state $1^1B_{1g}$ is 28,700 $cm^{-1}$, whereas ab initio calculations results 29,000 $cm^{-1}$. Note that in the ab initio case, the most important contribution (0.93) is from configuration $4b_{3g}4b_{2g}$. For other five g states ($2^1A_g$, $2^1B_{1g}$, $3^1A_g$, $3^1B_{1g}$, $4^1A_g$), the ab initio energies are on average $\sim$4500 $cm^{-1}$ higher as compared with our results. We also note that energies of both $1^1B_{3g}$ and $1^1B_{1u}$ $n\pi^*$ state come out very close in both calculations (35,600 and 36,100 viz. 35,300 and 36,600 $cm^{-1}$), but for other pair $n\pi^*$ states, $1^1B_{2g}$ and $1^1A_u$, the ab initio energies turn out to be lower by $\sim$6500 $cm^{-1}$. Also, our calculation results can be compared with those of work [33] in which full single and partial double configuration interaction on basis MO SCF CNDO/S method (CNDO/S-CISD) has been considered. Again the ordering of six g states both in our and CNDO/S-CISD calculations is practically identical. Only two pairs of levels—$2^1B_{1g}$, $3^1A_g$ and $3^1B_{1g}$, $4^1A_g$—have inverted position, but the energy gap between these levels within given pair is less than 300 $cm^{-1}$. The most pronounced difference between our CNDO/S-CIS and CNDO/S-CISD [33] calculations is in the large shifts down of all even $\pi\pi^*$ levels, from 3400 to 7800 $cm^{-1}$, which is very probably due to including of doubly excited configurations. It should be noted that lowest-lying excited $1^1B_{1g}$ level in the CNDO/S-CISD calculations is located below the $2^1B_{3u}$ ($B_x$) and $2^1B_{2u}$ ($B_y$) levels, by 700 and 2800 $cm^{-1}$, correspondingly.

As we continue to compare g parity states found in $H_2P$ and $H_2TPP$, following is also worth mentioning:

(i) In $H_2TPP$, the two lowest excited states, $1^1B_g$ and $2^1A_g$, the electronic density is mostly localization on the porphyrin fragment, with corresponding degree of localization, 95% and 92%. If one takes into account correspondence of MOs of $H_2P$ and $H_2TPP$ MOs (Table 1), then also the CIS contributions for these two states remains the same;

(ii) Unlike the u-parity levels ($Q_x$, $Q_y$, $B_x$, $B_y$ and $N_x$), $1^1B_g$ and $2^1A_g$ of $H_2TPP$ are practically not shifted as compared to $1^1B_{1g}$, $2^1A_g$ levels of $H_2P$. For $H_2TPP$ we find that the energy gap is, $\Delta E = E(2B_u) - E(1^1B_g) = -3000$ $cm^{-1}$, while for $H_2P$, $\Delta E = E(2^1B_{3u}) - E(1^1B_{1g}) = -2200$ $cm^{-1}$.

(iii) It was pointed out in Ref. [31] that the relative position of the first excited g level and $B_1$ (or $B_1$ and $B_2$) level(s) can be associated with the experimental observation of so-called blue fluorescence, which has been observed in tetrabenzoporphin free base [34,48,49], but was not registered for $H_2P$, as well as several other free base porphyrins. It was proposed that the blue fluorescence is due to transition(s) $B_1 \rightarrow G$ or $(B_1, B_2) \rightarrow G$. According to Ref. [32], such radiative transitions can occur when the first exited g level is higher in energy than $B_1$ ($B_1$, $B_2$) level(s). According to our result, going from $H_2P$ to $H_2TPP$ effectively lowers the levels $B_x$ and $B_y$, while the first excited g level ($1^1B_{1g}$ to $1^1B_g$) remains practically unchanged. If the above

considerations are correct, then this should lead to an increased blue fluorescence in $H_2TPP$;

(iv) One can find that the third g parity excited state in $H_2TPP$. $2^1B_g$, corresponds to $2^1B_{1g}$ state in $H_2P$. However, the degree of localization on the porphyrin fragment (79%) of $2^1B_g$ is notably lower than that for the $1^1B_g$ and $1^1A_g$ states of $H_2TPP$. The $2^1B_g$ level is lower by $\sim 1700\,cm^{-1}$, as compared to the $2^1B_{1g}$ level;

(v) In the higher energy region (above $33{,}000\,cm^{-1}$) we find a number of g parity energy levels. Similarly to the u parity states, they are composed by extensive mixing of local excitations and excitations with charge transfer between the porphyrin macrocycle and four phenyl rings.

In summary, the quantum-chemical calculations reveal for both $H_2P$ and $H_2TPP$ a series of g parity energy levels, which are situated near B states and higher. It is these states that should be considered as responsible ones for intense TPA in 365–395 nm region. As we already stated above, the extension of wavelength scanning to shorter wavelengths has been prevented by contribution of linear one-photon absorption by lowest Q state.

## 4. Conclusions

The detailed study of the two-photon absorption (TPA) for tetraphenylporphin free base has been carried out. TPA spectra and cross-sections were measured for $H_2TPP$ in toluene solution at room temperature. TPA in visible region corresponds to the transitions into pure electronic Q(0,0) state for $H_2TPP$ conformers without center of symmetry and to transitions into vibronic Q(0,1) state, which is allowed for all the conformers in solution. The transitions in UV region are attributed to parity allowed two-photon $g \rightarrow g$ transitions. The parity prohibition for two-photon transitions into pure electronic Q(0,0) state was proposed to be removed due to rotations of the phenyl rings promoting the loss of the center of inversion by $H_2TPP$ molecule. The higher value of two-photon cross-section found for the transition into vibronic Q(0,1) state, as compared with that for the transition into pure electronic Q(0,0) state, was explained by g parity of vibronic wavefunction. Measurements of the two-photon polarization ratio, $\Omega = \sigma_{circ}/\sigma_{lin}$, gave additional independent support for these assignments. Quantum-chemical calculations of u and g parity excited energy levels of $H_2TPP$ molecule were carried out by CNDO/S method. The importance of the exact molecular symmetry for the two-photon absorptivity into Q states was demonstrated. The results indicate that excited electronic states of g parity lie nearby B state and give rise to TPA bands in UV. In particular, two first g parity excited energy levels were found at practically the same energies for both $H_2P$ and $H_2TPP$, whereas u parity B states revealed energy decrease in going from $H_2P$ to $H_2TPP$.

## Acknowledgements

This work was supported by AFOSR grants F 49620-01-1-0406 and F 49620-01-1-0324.

## References

[1] W. Denk, J.H. Strickler, W.W. Webb, Science 248 (1990) 73.
[2] B.H. Cumpston, S.P. Ananthavel, S. Barlow, et al., Nature 398 (1999) 51.
[3] C.W. Spangler, J. Mater. Chem. 9 (1999) 2013.
[4] M. Drobizhev, A. Karotki, A. Rebane, Chem. Phys. Lett. 334 (2000) 76.
[5] A. Karotki, M. Kruk, M. Drobizhev, A. Rebane, J. Mod. Opt. 49 (2002) 379.
[6] K.D. Belfield, Spectrum 14 (2001) 1.
[7] E.A. Wachter, W.P. Partridge, E.G. Fisher, et al., Proc. SPIE 3269 (1998) 68.
[8] R.L. Goyan, D.T. Gramb, Photochem. Photobiol. 72 (2000) 821.
[9] S. Wan, J.A. Parrish, R.R. Anderson, M. Madden, Photochem. Photobiol. 34 (1981) 679.
[10] A. Karotki, M. Kruk, M. Drobizhev, A. Rebane, E. Nickel, C.W. Spangler, IEEE J. Sel. Top. Quantum Electron. 7 (2001) 971.
[11] M. Drobizhev, A. Karotki, M. Kruk, A. Rebane, Chem. Phys. Lett. 355 (2002) 175.
[12] R. Bonnet, Chem. Soc. Rev. 24 (1995) 19.

[13] K.M. Smith (Ed.), Porphyrins and Metalloporphyrins, Elsevier, Amsterdam, 1975, p. 910.
[14] M.J.S. Dewar, E.G. Zoebisch, E.F. Healey, J.J.P. Stewart, J. Am. Chem. Soc. 107 (1985) 3902.
[15] J.J.P. Stewart, MOPAC 6: a general molecular orbital package (QCPE 445), Frank J. Seiler Research Laboratory, US Air Force Academy, CO, 1990.
[16] B.M.L. Chen, A. Tulinsky, J. Am. Chem. Soc. 94 (1972) 4144.
[17] S.J. Silvers, A. Tulinsky, J. Am. Chem. Soc. 89 (1967) 3331.
[18] J. Del Bene, H.H. Jaffe, J. Chem. Phys. 48 (1968) 1807.
[19] R.L. Ellis, G. Kuehnlenz, H.H. Jaffe, Teor. Chim. Acta 26 (1972) 131.
[20] V.A. Kuzmitsky, Preprint of the Institute of Physics BSSR Academy of Science no. 188, 1979 (in Russian).
[21] A.V. Luzanov, Usp. Khim. 49 (1980) 2086 (in Russian).
[22] V.I. Bredikhin, M.D. Galanin, V.N. Genkin, Sov. Phys. Usp. 16 (1973) 299.
[23] D.W. Thomas, A.E. Martell, J. Am. Chem. Soc. 78 (1956) 1338.
[24] H.N. Fonda, J.V. Gilbert, R.A. Cormier, et al., J. Phys. Chem. 97 (1993) 7024.
[25] V.I. Gael, V.A. Kuzmitsky, K.N. Solovyov, Zh. Prikl. Spektrosk. 63 (1996) 932 (in Russian).
[26] N.N. Vsevolodov, L.P. Kostikov, L.P. Kayushin, V.I. Gorbatenkov, Biophysika (USSR Biophysics) 18 (1973) 755 (in Russian).
[27] K.N. Solovyov, L.L. Gladkov, A.S. Starukhin, S.F. Shkirman, Spektroskopiya porphyrinov: kolebatelnye sostojanija (Porphyrins Spectroscopy: Vibrational states), Nauka i Technika, Minsk, 1985, p. 416 (in Russian).
[28] R.R. Birge, B. Parsons, Q.W. Song, J.R. Tallent, in: M.A. Ratner, J. Jortner (Eds.), Molecular Electronics, Blackwell Science Ltd., Oxford, 1997, pp. 439–472.
[29] J. Rodriguez, C. Kirmaier, D. Holten, J. Am. Chem. Soc. 111 (1989) 6500.
[30] D. Magde, M.W. Windsor, D. Holten, M. Gouterman, Chem. Phys. Lett. 29 (1974) 183.
[31] S. Tobita, Y. Kaizu, H. Kobayashi, I. Tanaka, J. Chem. Phys. 81 (1984) 2962.
[32] V.A. Kuzmitsky, K.N. Solovyov, Zh. Prikl. Spektrosk. 27 (1977) 724 (in Russian).
[33] M.B. Masthay, L.A. Findsen, B.M. Pierce, D.F. Bocian, J.S. Lindsey, R.R. Birge, J. Chem. Phys. 84 (1986) 3901.
[34] V.A. Kuzmitsky, K.N. Solovyov, M.P. Tsvirko, in: N.S. Enikolopyan (Ed.), Porphyriny: spektroskopiya, elektrohimiya, primenenie (Porphyrins: Spectroscopy, Electrochemistry, Applications), Nauka, Moscow, 1987, pp. 7–126 (in Russian).
[35] H. Nakatsuji, J. Hasegawa, M. Hada, J. Chem. Phys. 104 (1996) 2321.
[36] V.A. Kuzmitsky, Zh. Prikl. Spektrosk. 68 (2001) 581 (in Russian).
[37] M. Drobizhev, A. Karotki, M. Kruk, N.Zh. Mamardashvili, A. Rebane, Chem. Phys. Lett. 361 (2002) 504.
[38] T.C. Wen, L.C. Hwang, W.Y. Lin, J. Chin. Chem. Soc. 49 (2002) 875.
[39] R. Birge, in: D. Kliger (Ed.), Ultrasensitive Laser Spectroscopy, Academic Press, New York, 1983, pp. 109–174.
[40] C.H. Reynolds, J. Org. Chem. 53 (1988) 6061.
[41] P. Bour, K. Zaruba, M. Urbanova, et al., Chirality 12 (2000) 191.
[42] F.A. Walker, G.N. La Mar, Ann. N. Y. Acad. Sci. 206 (1973) 328.
[43] M. Gouterman, in: D. Dolphin (Ed.), The Porphyrins, Vol. 3, Academic Press, New York, 1978, pp. 1–165.
[44] V.I. Gael, V.A. Kuzmitsky, K.N. Solovyov, Zh. Prikl. Spektrosk. 67 (2000) 696 (in Russian).
[45] G.M. Maggiora, L.J. Weimann, Chem. Phys. Lett. 22 (1973) 297.
[46] J.D. Backer, M.C. Zerner, Chem. Phys. Lett. 175 (1990) 192.
[47] L. Edwards, D.H. Dolphin, M. Gouterman, A.D. Adler, J. Mol. Spectrosc. 38 (1971) 16.
[48] L. Bajema, M. Gouterman, C.B. Rose, J. Mol. Spectros. 39 (1971) 421.
[49] V.N. Kotlo, K.N. Solovyov, S.F. Shkirman, Izvestiya AN SSSR (Bulletin of USSR Academy of Science), Seriya fizicheskaya 39 (1975) 1972 (in Russian).